Supplementary Information

Selective growth of layered perovskite for stable and efficient photovoltaics.

Kyung Taek Cho,[a] Giulia Grancini,[a] Yonghui Lee,[a] Emad Oveisi,[b] Jaehoon Ryu,[c] Osbel Almora,[d] Manuel Tschumi,[a] Pascal Alexander Schouwink,[e] Gabseok Seo,[f] Sung Heo,[g] Jucheol Park,[h] Jyongsik Jang,[c] Sanghyun Paek,[a]* Germà Garcia-Belmonte,[d] Mohammad Khaja Nazeeruddin[a]*

[a]Group for Molecular Engineering of Functional Materials, École Polytechnique Fédérale de Lausanne, Valais Wallis, CH-1951 Sion, Switzerland.

[b]Interdisciplinary Centre for Electron Microscopy, Ecole Polytechnique Fédérale de Lausanne, CH-1015 Lausanne, Switzerland.

[c]School of Chemical and Biological Engineering, Seoul National University, 599 Gwanangno, Gwanakgu, Seoul 151-742, Korea.

[d]Institute of Advanced Materials (INAM), Universitat Jaume I, 12006 Castelló, Spain

[e]Institut des Sciences et Ingénierie Chimiques, École Polytechnique Fédérale de Lausanne, Valais Wallis, CH-1951 Sion, Switzerland

[f]Department of Energy Science, Sungkyunkwan University, 2066, Seobu-ro, Jangan-gu, Suwon 16419, Korea

[g]Samsung Advanced Institute of Technology, 130, Samsung-ro, Yeongtong-gu, Suwon, 16678, Korea

[h]Business Support Department, Gumi Electrons & Information Technology Research Institute, Gumi, 39171, Korea

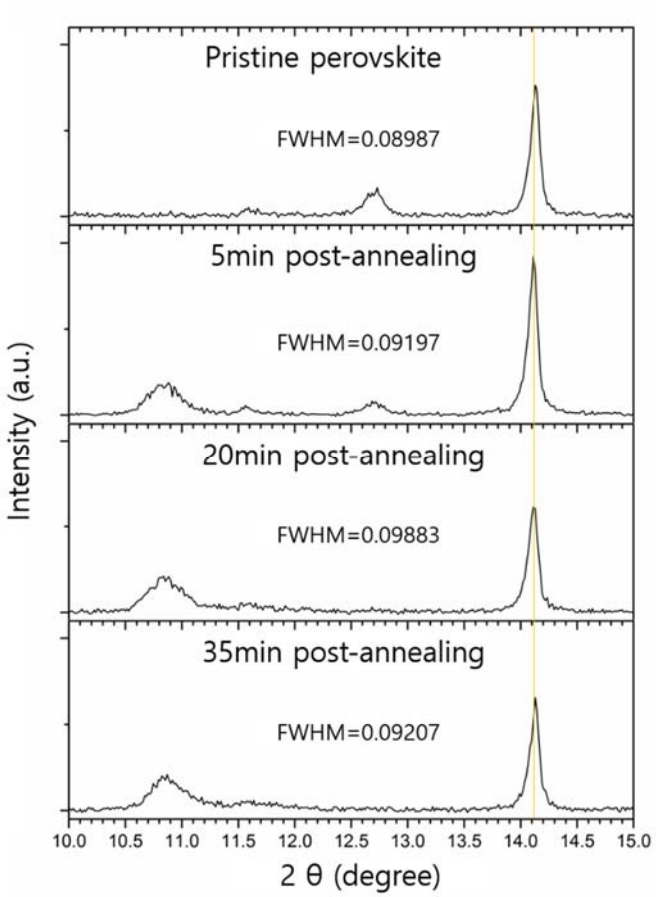

Figure S1. Magnified XRD data of region around 14°, the main 3D CFMPIB perovskite peak, as annealing time after spin coating PEAI isopropanol solution (10 mg/ml). Full-width at half-maximum of these CFMPIB perovskite peaks at 14.1° were calculated and listed.

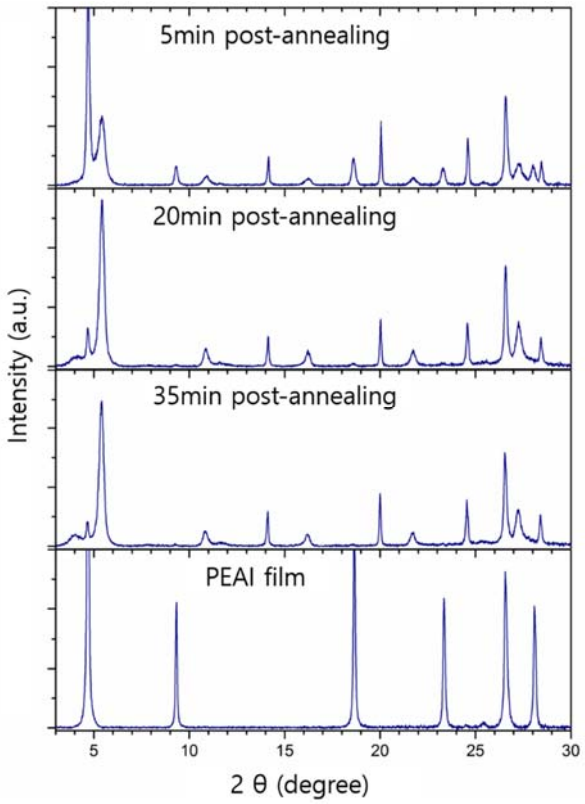

Figure S2. XRD spectra for L-CFM/P perovskite films varying annealing time (5, 20, and 30 min) and a PEAI film deposited on a TiO_2/FTO substrate by spin coating PEAI solution (15 mg/ml).

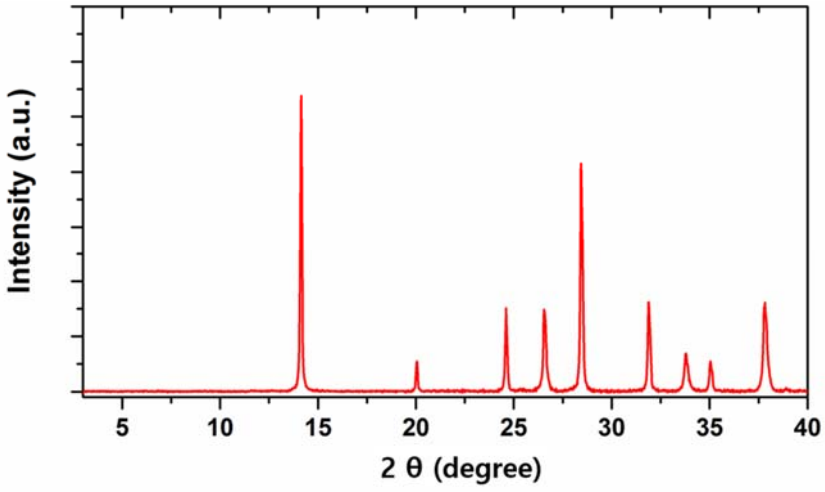

Figure S3. XRD spectra of a CFMPIB+PEAI perovskite film. For the CFMPIB+PEAI film, another precursor solution was prepared by adding PEAI to the CFMPIB precursor solution, where the amount of PEAI was same to the excess molar ratio of PbI_2 in the CFMPIB solution. The final composition of precursor solution was $PEA_{0.05}Cs_{0.1}FA_{0.73}MA_{0.13}PbI_{2.53}Br_{0.39}$. The perovskite film was fabricated by following same procedure for the CFMPIB perovskite film.

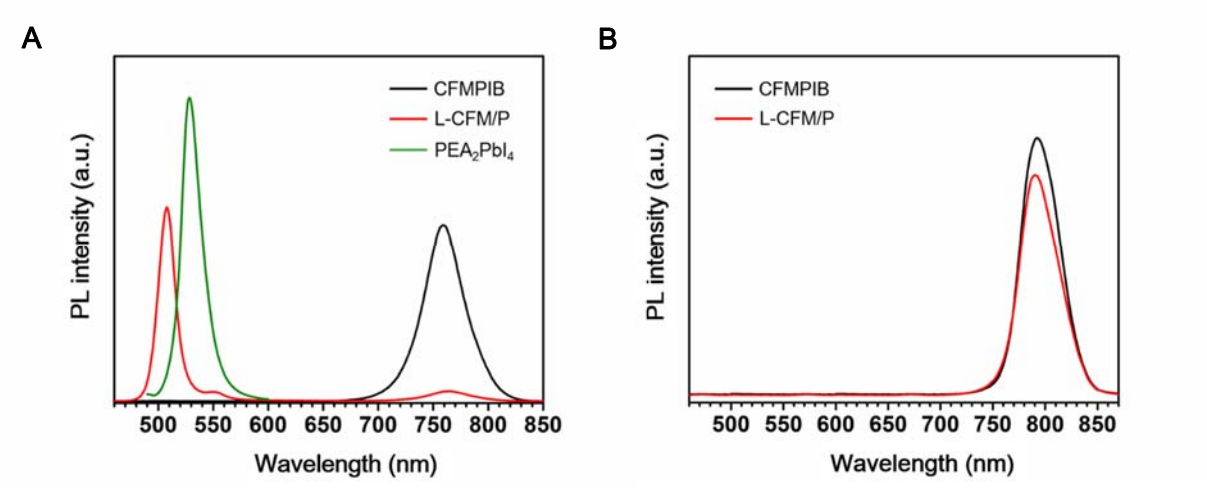

Figure S4. Steady-state PL spectra of CFMPIB, L-CFM/P, and PEA_2PbI_4 perovskite films. The intensity was not normalized and the PL emission peaks were obtained from top surface (A) and bottom side (B) of perovskite films. When prepared samples for (B), the perovskite films are coated on microscope glass for removing a quenching effect.

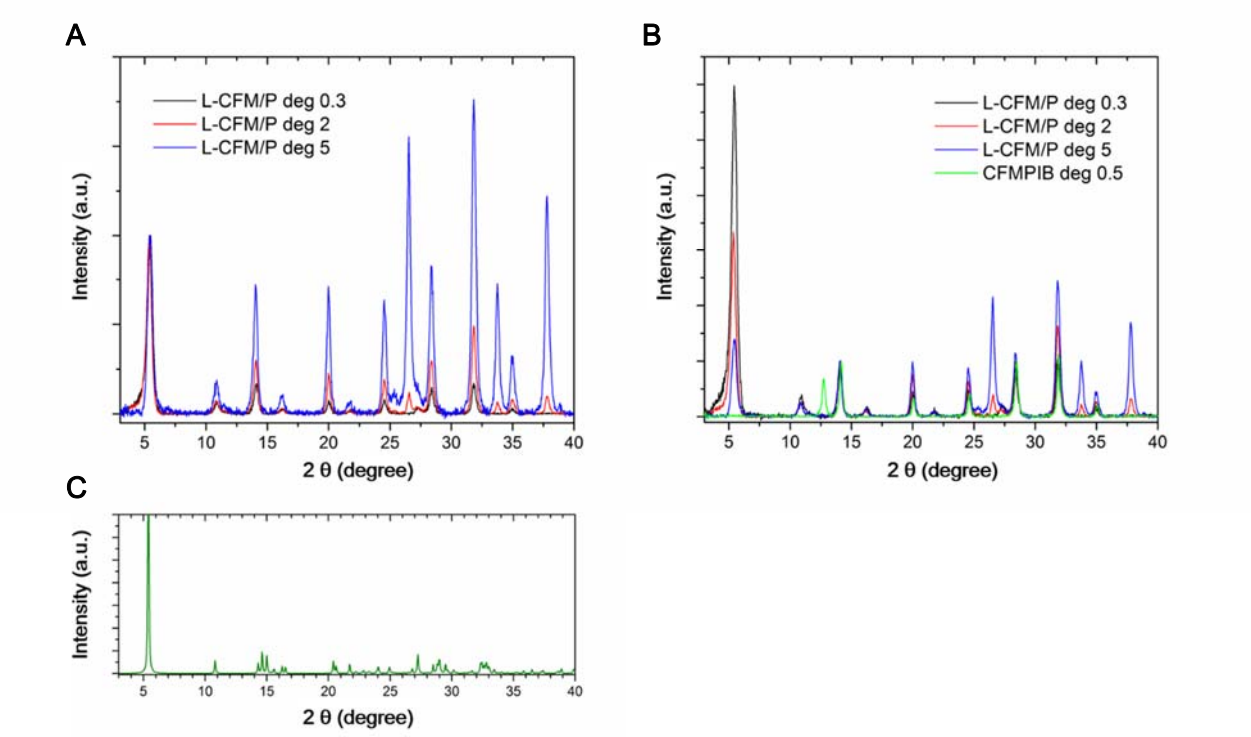

Figure S5. XRD measurement at fixed incident X-ray angle of 0.3°, 2°, and 5°. (A) XRD data were normalized to a main 2D perovskite (PEA_2PbI_4) peak of 5.44° 2θ. The relative signal intensity of the 3D phase at 14.1° increases with the incidence angle (blue - red - green curves). This indicates that the 2D perovskite is concentrated rather around the surface. Although we cannot tell how the layer is thick, it can be evidence that it is present in surface vicinity. (B) XRD data were normalized to a main 3D perovskite peak of 14.1°. (C) Calculated XRD data from PEA_2PbI_4 crystallographic information file obtained from a reference [1].

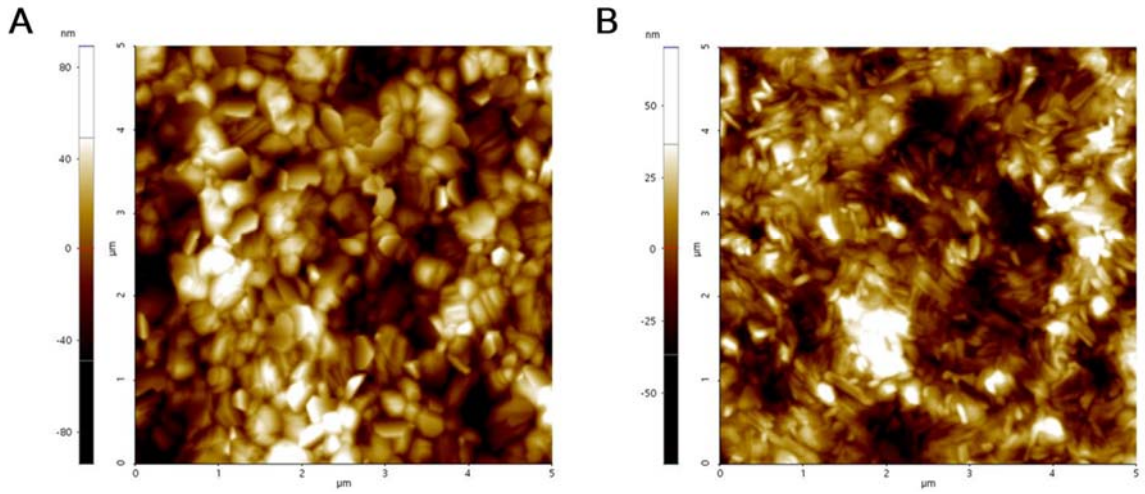

Figure S6. Comparison on roughness of perovskite films from typical AFM measurement. The AFM images of CFMPIB (A) and L-CFM/P (B) are taken as 5x5 um^2.

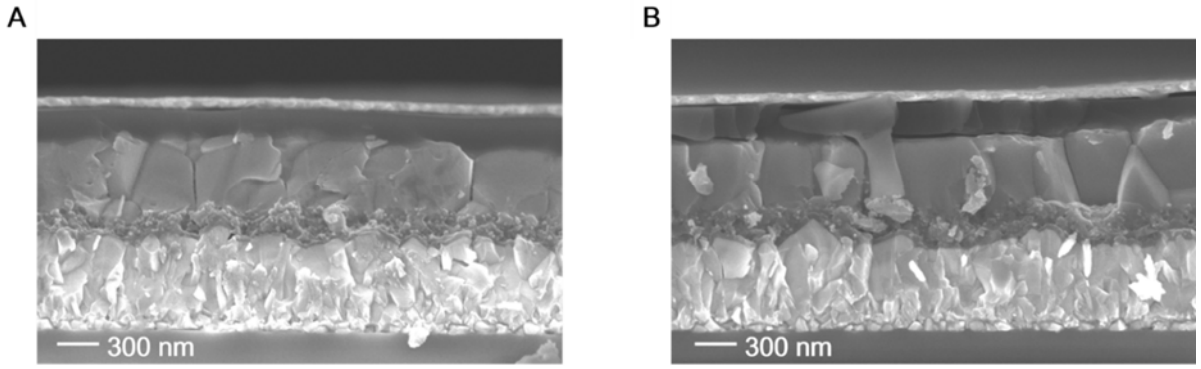

Figure S7. Cross-sectional SEM images of the complete devices fabricated with CFMPIB (A) and L-CFM/P (B).

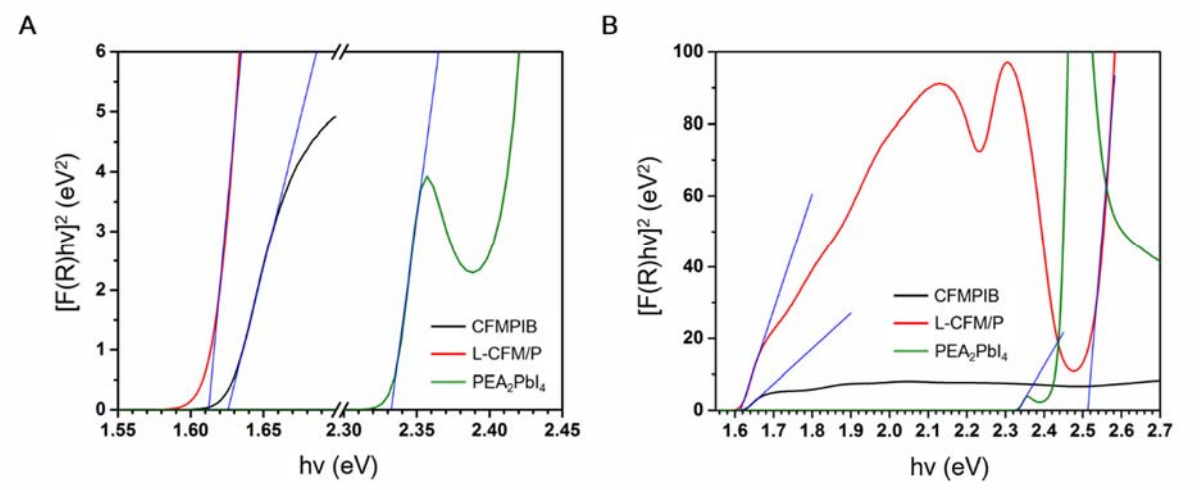

Figure S8. Tauc plot derived from reflectance spectra of CFMPIB, L-CFM/P, and PEA_2PbI_4 perovskite films assuming to direct band gap. (A) Magnified on intercept points and determination of optical band gaps. (B) Minimized to show the difference between CFMPIB and L-CFM/P.

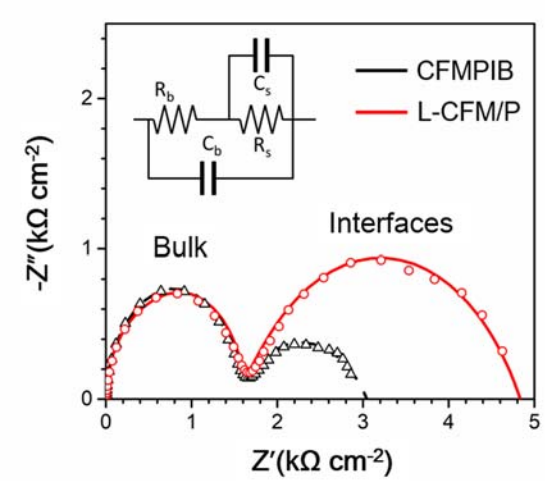

Figure S9. Open circuit impedance spectra with clear differences toward the low frequency range. The solid lines are fitted to the equivalent circuit of the inset. R_S and R_b represent resistance at surface and bulk, C_S and C_b represent capacitance at surface and bulk, respectively.

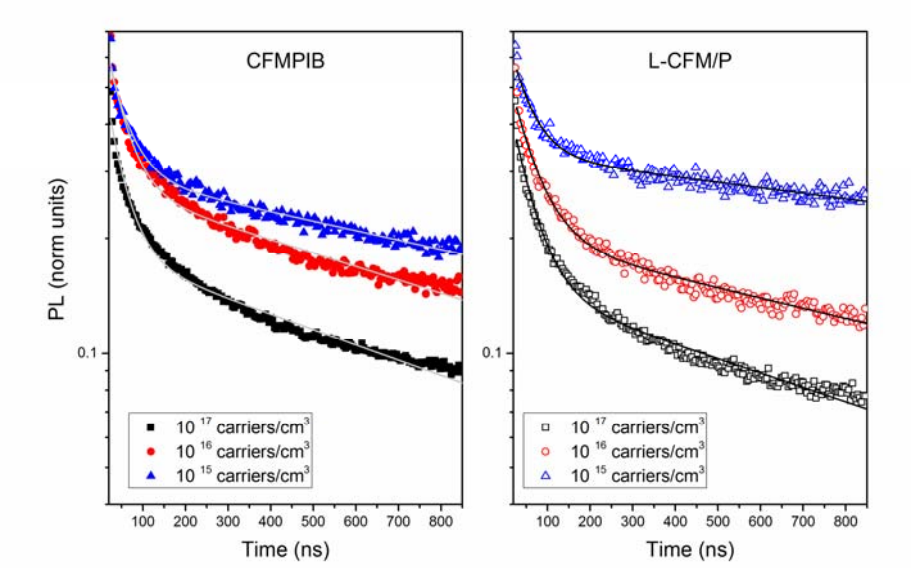

Figure S10. Time-resolved PL decays of CFMPIB and L-CFM/P perovskite films at different excitation densities from 10^{15} to 10^{17} carriers/cm^3. Samples have been encapsulated with a glass slide to prevent any oxygen induced degradation. The measurement was carried out by monitoring the PL from the top side of perovskite films at 770 nm.

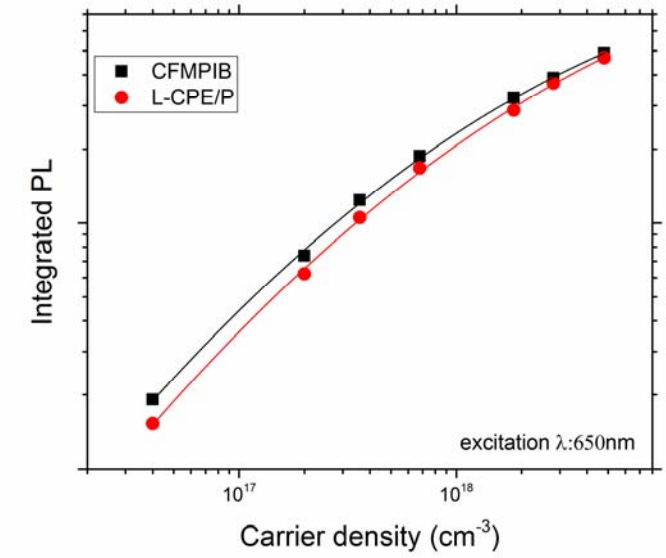

Figure S11. Time integrated Photoluminescence signal for the two perovskite as indicated in the legend as a function of the injected carrier density (cm^{-3}). Below 10^{17} cm^{-3} the integrated PL grows quadratically. So, the growth of PL signal with increasing pump fluence is dominated to the bimolecular radiative recombination rate; for the week pulse fluence corresponding to injected carrier density, the rate of carrier trapping is faster than the radiative recombination [2]. However, when this latter becomes faster than trapping at above 10^{17} cm^{-3}, the PL signal saturates and quantum yield (integrated PL/pulse fluence) will decrease by resulting from non-radiative recombination. In here, two perovskite films show similar behaviours at saturation point and the rate of growth. We can conclude the effect of trap density in two perovskite will be little difference.

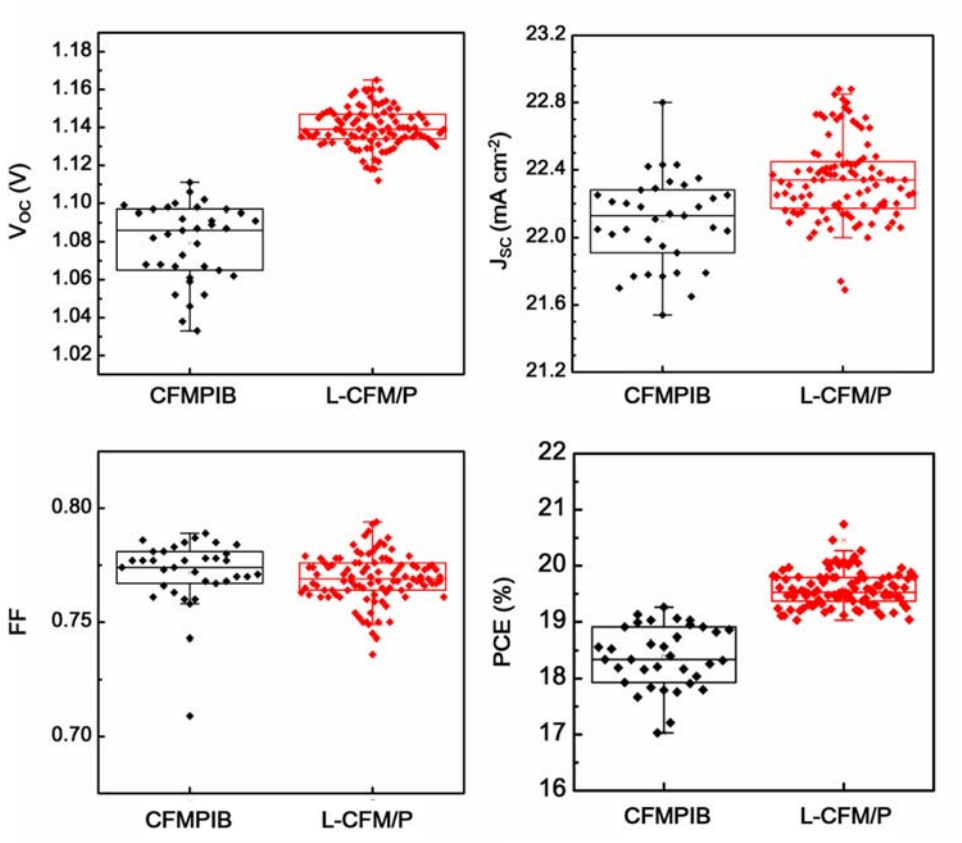

Figure S12. Statistics of V_{OC}, J_{SC}, FF, and PCE of devices more than 100. Showing that the main reason behind upgrading PCE lies in the V_{OC} improved from 1.08 to 1.14 V, which can be associated with a significant recombination reduction. With respect to the J_{SC}, a scattered ~0.2 mA cm^{-2} larger photocurrents were obtained for 2D/3D structures.

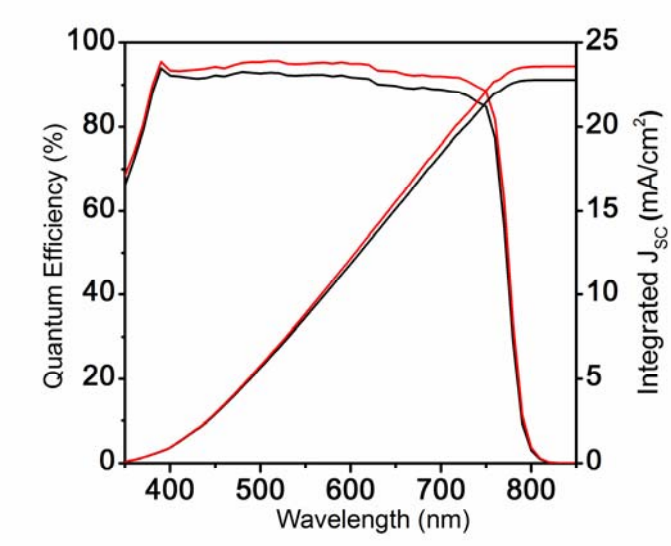

Figure S13. IPCE spectrums and integrated J_{SC} from IPCE.

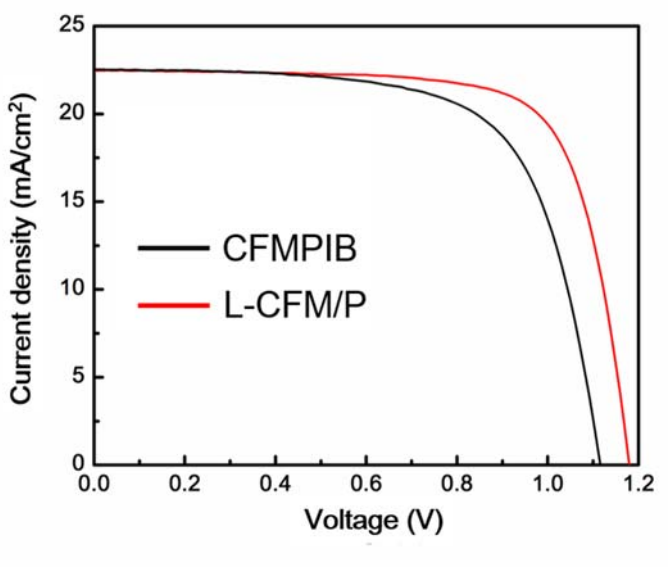

Figure S14. J-V curves of devices based on SnO_2 with CFMPIB and L-CFM/P perovskite.

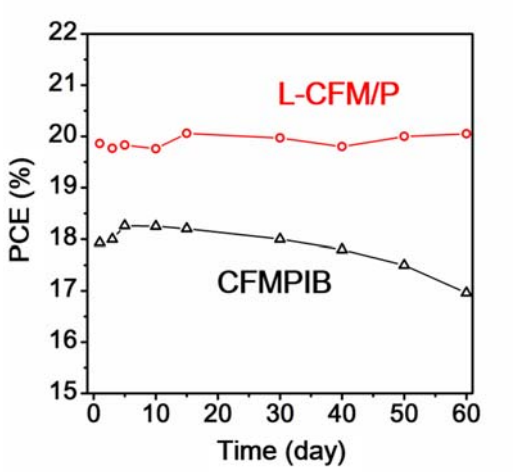

Figure S15. Dark storage stability of devices with CFMPIB and L-CFM/P. All of cells are stored in dark and measured in ambient atmosphere.

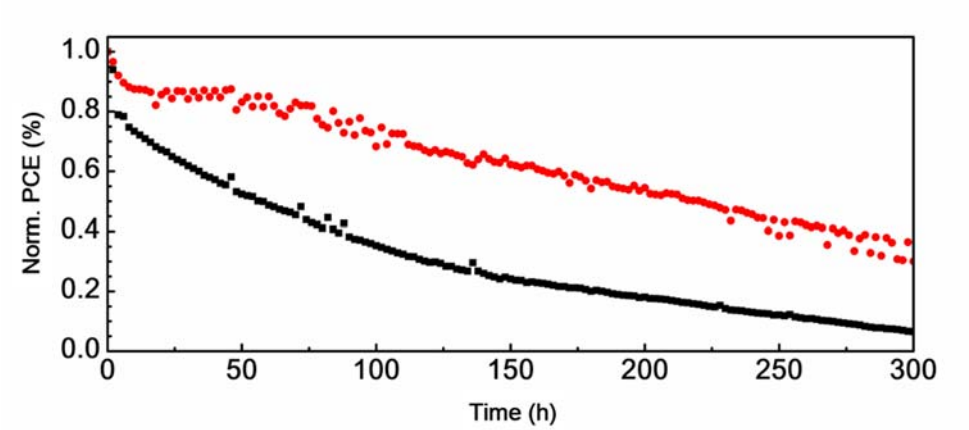

Figure S16. PCE tracking from J-V measurement for 300 h of unencapsulated devices with CFMPIB (black) and L-CFM/P (red) under continuous flowing humid air gas and full-sun illumination.

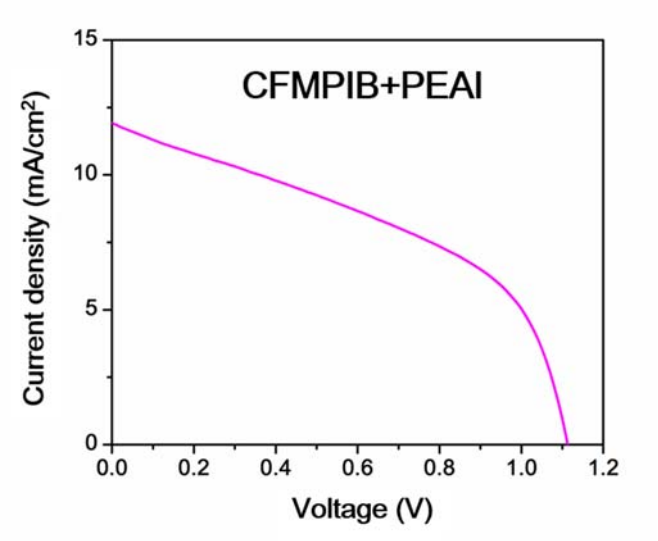

Figure S17. J-V curve of a homogeneous perovskite mixture of CFMPIB+PEAI device.

Table. S1 Decay lifetime from PL fitting in Figure S10

	10^{15} carrier/cm^3		10^{16} carrier/cm^3		10^{17} carrier/cm^3	
	τ_1	τ_2	τ_1	τ_2	τ_1	τ_2
CFMPIB	36	790	41	>800	34	>800
L-CFM/P	29	749	31	>800	33	>800

1. K.-z. Du, Q. Tu, X. Zhang, Q. Han, J. Liu, S. Zauscher and D. B. Mitzi, *Inorganic Chemistry*, 2017, **56**, 9291-9302.
2. M. Saba, M. Cadelano, D. Marongiu, F. Chen, V. Sarritzu, N. Sestu, C. Figus, M. Aresti, R. Piras, A. Geddo Lehmann, C. Cannas, A. Musinu, F. Quochi, A. Mura and G. Bongiovanni, 2014, **5**, 5049.